

Preparation and electrochemical performance of Na-doped $\text{Li}_3\text{V}_2(\text{PO}_4)_3/\text{C}$ cathode material

Ji Yan · Wei Yuan · Hui Xie · Zhi-yuan Tang ·
Fu-jun Liu · Wen-feng Mao · Qiang Xu · Xin-he Zhang

Received: 15 September 2011 / Revised: 16 March 2012 / Accepted: 28 April 2012 / Published online: 10 May 2012
© Springer-Verlag 2012

Abstract Na-doped $\text{Li}_3\text{V}_2(\text{PO}_4)_3/\text{C}$ (LVP/C) cathode materials are prepared by a sol–gel method. X-ray diffraction results show that the Na ion has been well doped into the crystal structure of LVP/C and does not disturb the extraction–insertion behavior of lithium ion seriously. The initial discharge capacity of the Na-doped LVP/C is $112.2 \text{ mA h g}^{-1}$ at 5 C, and the capacity retention reaches 98.3 % over 80 cycles. Cyclic voltammetry and electrochemical impedance spectra indicate that the reversibility of electrochemical redox reaction and the charge-transfer resistance of LVP/C cathode material have been significantly improved by Na doping. The improved performances can be attributed to the more convenient route for lithium ion diffusion and the lower activation energy of the extraction–insertion of lithium ion due to the weakness of Li–O bond.

Keywords Li-ion battery · Sol–gel process · Powder diffraction · Electrochemical properties

J. Yan (✉) · W. Yuan · Z.-y. Tang · W.-f. Mao · Q. Xu
Department of Applied Chemistry, Tianjin University,
Tianjin 300072, China
e-mail: jiyang@tju.edu.cn

H. Xie
Materials Science and Engineering Program,
University of Texas at Austin,
Austin, TX 78712, USA

F.-j. Liu
Department of General, Organic and Biomedical Chemistry,
NMR and Molecular Imaging Laboratory, University of Mons,
Avenue Maistriau, 19,
7000 Mons, Belgium

X.-h. Zhang
McNair Technology Co., Ltd.,
Dongguan, Guangdong 523800, China

Introduction

Recently, lithium vanadium phosphate ($\text{Li}_3\text{V}_2(\text{PO}_4)_3$) with monoclinic structure is investigated extensively as a promising candidate cathode material for lithium ion batteries [1]. $\text{Li}_3\text{V}_2(\text{PO}_4)_3$ possesses several advantages including high theoretical capacity (197 mA h g^{-1}), desirable discharge voltage plateau (4.1 V), high-rate capability, and superior cycling stability [2–5]. However, the poor electronic conductivity and ion transferability hinder the practical application of $\text{Li}_3\text{V}_2(\text{PO}_4)_3$, especially in the field of high-power lithium ion batteries [6]. To overcome these intrinsic drawbacks, various approaches have been adopted via coating a carbon layer [7, 8], reducing the particle size [9, 10], and doping a foreign metal ion [11–13]. Normally, the substitution of a foreign metal ion always occurred at V-site resulting in an improved electrochemical performance and the enhancement of intrinsic electronic conductivity.

It is well known that Na has been widely used as a substitute for lithium to improve the electronic conductivity and ionic transportation of lithium metal compound. Ouyang et al. [14] employ the first-principle calculation to study the influence of Na doping on electronic structure and ionic dynamic properties of LiFePO_4 . The results indicate that Na doping not only greatly facilitates the electron conductivity but also benefits the lithium ion migration of LiFePO_4 . Additionally, Yin et al. [15] have successfully synthesized the Na-doped LiFePO_4/C composites and investigated the high-rate performance and cyclic stability. For lithium vanadium phosphates, Cushing et al. [16] have synthesized $\text{Li}_2\text{NaV}_2(\text{PO}_4)_3$ samples as 3.7 V lithium-insertion cathode materials with rhombohedral NASICON structure via ion exchange from $\text{Na}_3\text{V}_2(\text{PO}_4)_3$ and investigated their structural characteristics and electrochemical performances. Recently, Kuang et al. [17] and Chen et al. [18] independently investigate the effect of partial

substitution of Na ion on the electrochemical performance of $\text{Li}_3\text{V}_2(\text{PO}_4)_3$. In the potential range of 3.0 to 4.8 V, the $\text{Li}_{2.95}\text{Na}_{0.05}\text{V}_2(\text{PO}_4)_3/\text{C}$ composite prepared by Chen et al. presents $153.4 \text{ mA h g}^{-1}$ at 1-C rate, and the $\text{Li}_{2.97}\text{Na}_{0.03}\text{V}_2(\text{PO}_4)_3/\text{C}$ material synthesized by Kuang et al. delivers $118.9 \text{ mA h g}^{-1}$ at 2-C rate.

In this study, Na-doped $\text{Li}_3\text{V}_2(\text{PO}_4)_3/\text{C}$ (LVP/C) cathode materials were synthesized via a sol–gel method and the effects of partial substitution of Na at Li site on the rate capability and cyclic stability of LVP/C were also investigated. Different from the above two literatures of Na-doped $\text{Li}_3\text{V}_2(\text{PO}_4)_3$, we investigated here the positive effect of Na doping on the electrochemical performance of $\text{Li}_3\text{V}_2(\text{PO}_4)_3/\text{C}$ in the potential range of 3.0 to 4.3 V. The high-rate capability of the as-synthesized composite was also investigated. Furthermore, the relationship of crystal structure, morphology, and high-rate capability between pristine LVP/C and Na-doped LVP/C composites was discussed in detail.

Experimental

The Na-doped $\text{Li}_3\text{V}_2(\text{PO}_4)_3/\text{C}$ cathode materials were synthesized by a sol–gel method. Stoichiometric amounts of Li_2CO_3 , V_2O_5 , $\text{NH}_4\text{H}_2\text{PO}_4$, and NaNO_3 were dissolved in distilled water with continuous stirring for 5 h at room temperature to obtain a clear solution. Then, a certain amount of citric acid solution was slowly added into the mixture with vigorous stirring. Herein, the amount of citric acid was determined by the residual carbon content in the final products. Then, *pH* of the solution was adjusted to 9 by ammonized water. After stirring for 3 h at room temperature, the resulting sol was evaporated at 80°C and heated at 120°C for 12 h to achieve a dry gel. Subsequently, the dry gel precursors were precalcined at 350°C for 4 h to decompose carbonate and ammonium under N_2 gas atmosphere. Finally, the as-prepared precursors were reground, pelletized, and calcined at 850°C for 8 h under flowing N_2 gas to yield Na-doped LVP/C composites. The amount of residual carbon in LVP/C composites was measured to be about 6.5 %, which is based on the method used in the previous literature [19]. For comparison, the pristine LVP/C was also prepared in the same process without using NaNO_3 .

The crystalline and structural analyses of the composites were performed by powder X-ray diffraction (XRD, Bruker D8 diffractometer) using *Cu-K α* radiation from 10° to 60° at a scanning rate of $0.02^\circ \text{ s}^{-1}$. The morphology and particle size of the samples were observed with a scanning electron microscope (SEM, JSM-7001F).

The electrochemical performances of the samples were measured by using 2023-type coin cells. The cathode electrodes were fabricated by mixing the as-synthesized Na-doped LVP/C (80 %) or the pristine one with super P (10 %) and

polytetrafluoroethylene (60 wt%) binder (10 %). After drying at 120°C for 12 h in a vacuum oven, the obtained electrodes were cut into disk-shaped flakes with a diameter of about 8 mm. The coin cells were assembled in a Mikrouna glove box filled with high-purity argon using lithium metal foil as the counter electrode and 1 M LiPF_6 in ethylene carbonate–dimethyl carbonate (1:1, by volume ratio) as the electrolyte. The electrochemical galvanostatically charged and discharged testing was performed between 3.0 and 4.3 V at room temperature by utilizing a battery tester (NEWARE, BTS-610, Shenzhen, China) and by applying a rate of 0.2 to 5 C. Cyclic voltammogram tests (CVs) were conducted from 3.0 to 4.5 V with a sweep rate of 0.1 mV s^{-1} . Electrochemical impedance spectra measurements were recorded using a Gamry electrochemical workstation with an AC voltage signal of 5 mV in the frequency range of 10^5 to 0.01 Hz, based on the similar electrode area and active-material loading.

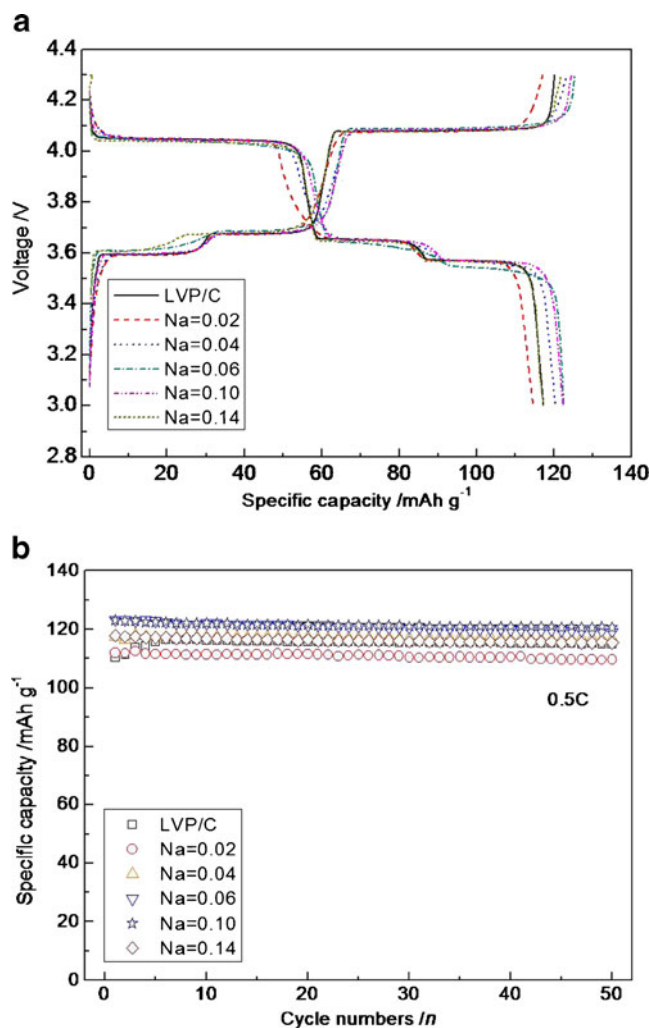


Fig. 1 The typical charge and discharge curves of the pristine LVP/C and Na-doped LVP/C (Na = 0.00, 0.02, 0.04, 0.06, 0.1, and 0.14) composites at 0.2-C rate (a) and the prolonged cycling performance at 0.5-C rate (b)

Results and discussion

Figure 1 shows the initial charge–discharge curves of the Na-doped LVP/C composites at various Na-doping amounts of 0.00, 0.02, 0.04, 0.06, 0.10, and 0.14 in the potential range of 3.0–4.3 V at 0.2 C. Three pairs of redox voltage plateaus around 3.59/3.58, 3.67/3.66, and 4.08/4.06 V can be observed for all the samples, which correspond well to the extraction and intercalation process of two lithium ions, accompanying with a two-step phase transition process of $\text{Li}_x\text{V}_2(\text{PO}_4)_3$ from $x=3.0$ to 2.5, 2.0, and 1.0 [1]. As shown in the figure, an increase of discharge capacity is obtained for most Na-doped composites except Na = 0.02 sample. This indicates that the Na doping does not block the diffusion tunnel of lithium ion which can be ascribed to the pillar effect of Na ions, as reported in Na-doped LiFePO_4 [15] and Na-doped $\text{Li}_3\text{V}_2(\text{PO}_4)_3$ [17]. On the other hand, the increased specific capacities for Na-doped composites may be caused by the depressed impedance of lithium ion diffusion resulting from the weakness of Li-O bond [17]. For the pristine one, the specific discharge capacity is $110.42 \text{ mA h g}^{-1}$ at 0.5-C rate and reaches $114.91 \text{ mA h g}^{-1}$ after 50 cycles. In contrast, the Na-doped composite of Na = 0.10 delivers a higher specific discharge capacity of $120.57 \text{ mA h g}^{-1}$ and a slight capacity decay of 2.62 mA h g^{-1} is detected over 50 cycles. It is believed that Na doping cannot only improve the specific discharge capacity and electron conductivity of LVP but also stabilize the crystal structure to achieve more excellent cycling performance, as predicted by Ouyang et al. [14]. From the above results, we confirm that the Na doping amount of 0.10 is the optimal amount and is assigned as Na-doped LVP/C (Na = 0.10) in the following experiments.

In order to identify the crystal structure difference between the pristine LVP/C and Na-doped LVP/C (Na = 0.10),

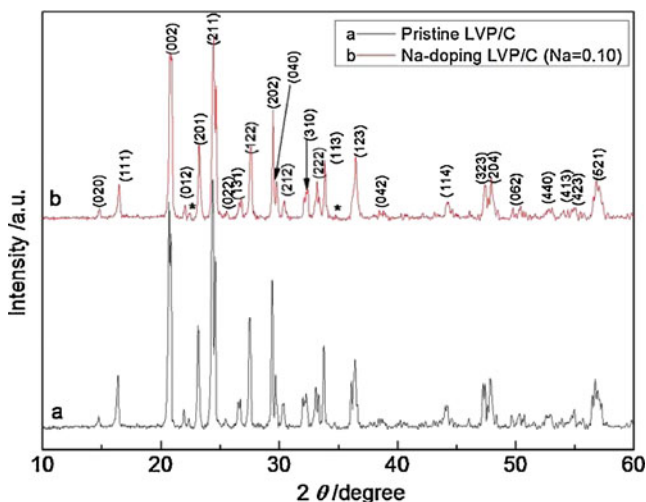


Fig. 2 XRD patterns of the pristine LVP/C (a) and Na-doped LVP/C (Na = 0.10) (b) composites

Table 1 Lattice parameters of the pristine LVP/C (a) and Na-doped LVP/C (Na = 0.10) composite

Samples	<i>a</i> (Å)	<i>b</i> (Å)	<i>c</i> (Å)	<i>V</i> (Å ³)	<i>R</i> (%)
Pristine LVP/C	8.546	11.985	8.592	880.09	16.18
Na-doped LVP/C (Na = 0.10)	8.605	11.972	8.656	891.74	19.88

X-ray diffraction analysis is performed and the results are shown in Fig. 2. The sharp peaks of two samples indicate good crystallinity of both composites. We also have detected the unknown peaks in the XRD pattern and added the impurity phase peaks of Li_3PO_4 . Furthermore, no any peak of crystalline carbon is observed, indicating that the coating carbon on LVP particle is amorphous. The Jade 5 software is used to study the influence of Na doping on lattice parameters of the LVP/C composites. As shown in Table 1, the *a*- and *c*-axis are expanded and *b*-axis is shrunk with the

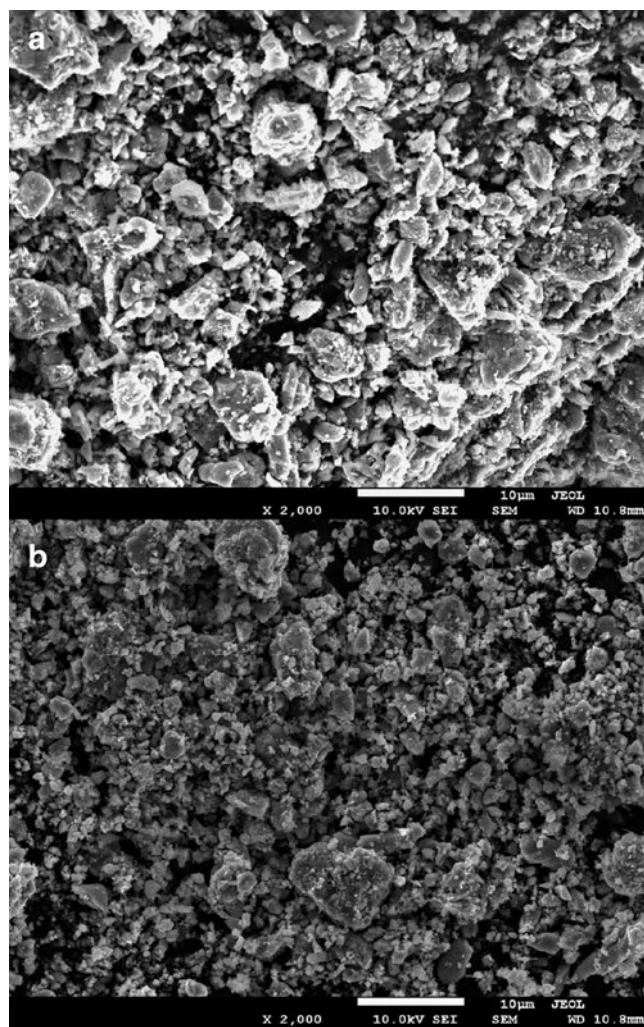


Fig. 3 SEM images of the pristine LVP/C (a) and Na-doped LVP/C (Na = 0.10) (b) composites

overall volume increasing after Na doping, demonstrating that the doped Na ion has taken up the lithium site (Li3(4e)) and a uniform solid solution is formed, which is almost consistent with the recent report by Kuang et al. [17] and Chen et al. [18]. The good doping effect is closely related to the homogeneous mixing of metal ions at atomic level by using the sol–gel method. The expanded cell volume is mainly attributed to the larger ion radius of Na^+ (1.02 Å) than Li^+ (0.76 Å) [20].

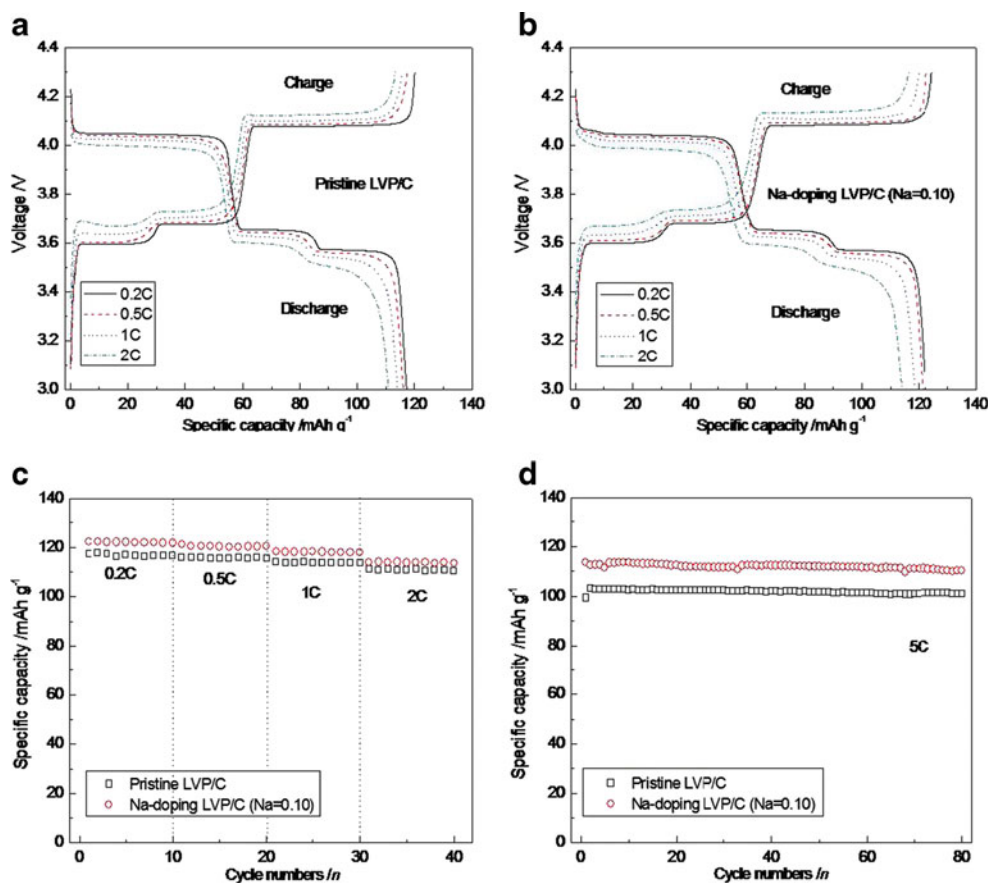
Scanning electron micrographs of the pure and Na-doped LVP/C ($\text{Na} = 0.10$) composites are shown in Fig. 3. It can be seen that a wide particle size distribution ranges from 4 to 8 μm with some agglomerated particles congregation for pristine LVP/C (Fig. 3a). In comparison, the Na-doped LVP/C ($\text{Na} = 0.10$) composite is composed of smaller particles (0.5–2 μm) with a comparative uniform morphology (Fig. 3b).

The rate performances of the pristine LVP/C and Na-doped LVP/C ($\text{Na} = 0.10$) are compared in Fig. 4. For the pristine sample (Fig. 4a), a specific capacity of 117.3 mA h g^{-1} is obtained at 0.2-C rate and the value maintains about 94.64 % after increasing the rate to 2 C. In comparison, the Na-doped LVP/C ($\text{Na} = 0.10$) delivers 122.3 mA h g^{-1} at 0.2 C and retains 113.95 mA h g^{-1} by increasing the rate from 0.2 to 2 C. When the rate increases from 2 to 5 C (Fig. 4b), there is a

significant difference in the specific capacity between the pristine and Na-doped LVP/C ($\text{Na} = 0.10$). It can be seen that 113.56 mA h g^{-1} of the specific discharge capacity and 99.40 % of the capacity retention are obtained for Na-doped LVP/C ($\text{Na} = 0.10$), while the pristine LVP/C only retains 100.98 mA h g^{-1} after 80 cycles. The faster lithium ion migration and the better particle distribution via a sol–gel method are responsible for the obtained high-rate performance after Na doping. The above results suggest that at higher rate (5 C), the electrochemical dynamics may be determined by the Li^+ diffusion in the bulk of material rather than the electrochemical reaction rate.

Figure 5 shows the cyclic voltammogram curves of the pristine LVP/C and Na-doped LVP/C ($\text{Na} = 0.10$) at a scanning rate of 0.1 mV s^{-1} between 3.0 and 4.5 V. Both curves exhibit a similar profile. Three oxidation peaks and three reduction peaks can be observed for both samples, occurring at 3.64, 3.73, and 4.15 V for oxidation reaction and three corresponding reduction reactions occurring at 3.52, 3.59, and 3.97 V. The results are in good agreement with the report by Säidi et al. [21]. After Na doping, the potential separation (ΔE_s) decreases significantly for all the three redox peaks, suggesting the enhancement of electrochemical reversibility. The decrease of the ΔE_s may due to the weakness of the Li-O bond and the expandable lithium

Fig. 4 **a** The charge–discharge curves of the pristine LVP/C and **b** Na-doped LVP/C ($\text{Na} = 0.10$) composites at various rates; **c** the corresponding cycling performances and **d** 5-C rate cycling life



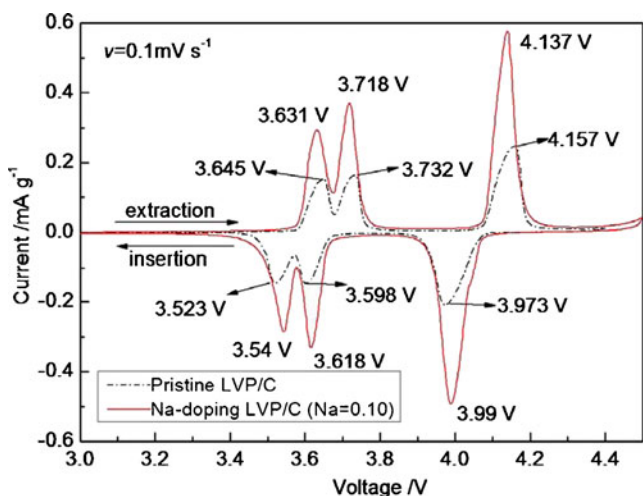


Fig. 5 CV curves of the pristine LVP/C and Na-doped LVP/C (Na = 0.10) composites at a scanning rate of 0.1 mV s⁻¹ between 3.0 and 4.5 V at room temperature

diffusion tunnel after Na-doping, which is beneficial for high-rate capability and cycling performance of LVP/C cathode material.

The electrochemical impedance spectra measurements were measured to understand the kinetic process of the pristine LVP/C and Na-doped LVP/C (Na = 0.10) (Fig. 6). The inset equivalent circuit is used to simulate the impedance spectra. It is observed that both electrodes exhibit a semicircle in the high frequency and an inclined line in the low frequency. The high-frequency semicircle corresponds to the solution resistance (R_c). The middle frequency semicircle is attributed to the charge-discharge process, which may consist with the charge-transfer resistance, particle-to-particle resistance (R_1), and double-layer capacitance (CPE_1), whereas the low frequency

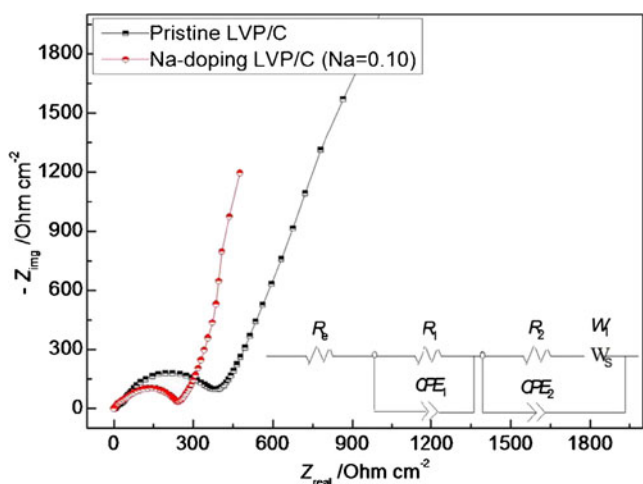


Fig. 6 Nyquist plots of the pristine LVP/C and Na-doped LVP/C (Na = 0.10) composites at unactivation state. *Inset*: Equivalent circuit corresponding to the impedance diagrams

semicircle represents the diffusion of lithium ion in the bulk of the electrode and this process is connected with the surface film and charge-transfer resistance (R_2), CPE_2 , and Warburg impedance (W_1). As shown in Fig. 6, the charge-transfer resistance of the Na-doped composite is lower than that of the pristine, which also can be due to the increase of electron conductivity associated with the expandable lithium-ion transfer tunnel.

Conclusion

In this study, the pristine and Na-doped LVP/C composites are synthesized by a sol-gel method. The investigation of the influence of Na doping on the structural and electrochemical characteristics of LVP/C composite shows that the Na ion has been well solved into the crystal structure of LVP/C and the resulting composite exhibits smaller particle size, lower electron-transfer resistance, and faster lithium ion migration, which are attributed to the expanded lithium ion transfer tunnel by Na doping. Furthermore, the Na-doped LVP/C (Na = 0.10) composite delivers a higher specific capacity of 112.2 mA h g⁻¹ with excellent rate capability (5-C rate) and cycling stability. Based on the above studies, we confirm that a high-rate performance of LVP/C cathode material can also be obtained by Na doping.

Acknowledgments This study was supported by the National Science Foundation of China (grant no. 20973124) and Guangdong Science and Technology Key Projects (grant no. 2009A080208001).

References

- Huang H, Yin SC, Kerr T, Taylor N, Nazar LF (2002) Adv Mater 14:1525–1528
- Qiao YQ, Wang XL, Xiang JY, Zhang D, Liu WL, Tu JP (2011) Electrochim Acta 56:2269–2275
- Rui XH, Jin Y, Feng XY, Zhang LC, Chen CH (2011) J Power Sources 196:2109–2114
- Qiao YQ, Tu JP, Wang XL, Gu CD (2012) J Power Sources 199:287–292
- Zhang X, Guo H, Li X, Wang Z, Wu L (2012) Electrochim Acta 64:65–70
- Qiao YQ, Tu JP, Wang XL, Zhang D, Xiang JY, Mai YJ, Gu CD (2011) J Power Sources 196:7715–7720
- Barker J, Saidi MY, Swoyer JL (2003) J Electrochem Soc 150: A684–A688
- Yuan W, Yan J, Tang ZY, Sha O, Wang JM, Mao WF, Ma L (2012) J Power Sources 201:301–306
- Pan AQ, Choi DW, Zhang JG, Liang SQ, Cao GZ, Nie ZM, Arey BW, Liu J (2011) J Power Sources 196:3646–3649
- Wang LJ, Tang ZY, Ma L, Zhang XH (2011) Electrochem Commun 13:1233–1235
- Ai DJ, Liu KY, Lu ZG, Zou MM, Zeng DQ, Ma J (2011) Electrochim Acta 56:2823–2827

12. Deng C, Zhang S, Yang SY, Gao Y, Wu B, Ma L, Fu BL, Wu Q, Liu FL (2011) *J Phys Chem C* 115:15048–15056
13. Xia Y, Zhang WK, Huang H, Gan YP, Li CG, Tao XY (2011) *Mater Sci Eng B* 176:633–639
14. Ouyang CY, Wang DY, Shi SQ, Wang ZX, Li H, Huang XJ, Chen LQ (2006) *Chin Phys Lett* 23:61–64
15. Yin XG, Huang KL, Liu SQ, Wang HY, Wang H (2010) *J Power Sources* 195:4308–4312
16. Cushing BL, Goodenough JB (2001) *J Solid State Chem* 162:176–181
17. Kuang Q, Zhao YM, Liang ZY (2011) *J Power Sources* 196:10169–10175
18. Chen QQ, Qiao XC, Wang YB, Zhang TT, Peng C, Yin WM, Liu L (2012) *J Power Sources* 201:267–273
19. Rui XH, Li C, Liu J, Cheng T, Chen CH (2010) *Electrochim Acta* 55:6761–6767
20. Park SH, Shin SS, Sun YK (2006) *Mater Chem Phys* 95:218–221
21. Saidi MY, Barker J, Huang H, Swoyer JL, Adamson G (2002) *Electrochem Solid-State Lett* 5:A149–A151